NeuroImage: Clinical 24 (2019) 102010

Contents lists available at ScienceDirect

NeuroImage: Clinical

journal homepage: www.elsevier.com/locate/ynicl

Resting state network plasticity related to picture naming in low-grade glioma patients before and after resection

L.E.H. van Dokkum[a,b,*], S. Moritz Gasser[c,d], J. Deverdun[a,b], G. Herbet[c,d], T. Mura[e], B. D'Agata[e], M.C. Picot[e], N. Menjot de Champfleur[a,b,f], H. Duffau[c,d], F. Molino[a,f], E. le Bars[a,b]

[a] I2FH, Institut d'Imagerie Fonctionelle Humaine, Montpellier University Hospital, Gui de Chauliac, 80 av. Augustin Fliche, 34295 Montpellier, France
[b] Neuroradiology Department, Montpellier University Hospital, Gui de Chauliac, France
[c] Neurosurgery Department, Montpellier University Hospital, Gui de Chauliac, France
[d] Team 'Plasticity of Central Nervous System, Stem Cells and Glial Tumors', INSERM U1051, Institute of Neuroscience Montpellier, France
[e] Epidemiology Department, Clinical Investigation Center, INSERM-CIC 1411, Montpellier University Hospital, France
[f] Laboratoire Charles Coulomb, Montpellier University, France

ARTICLE INFO

Keywords:
Resting state
Glioma
Neurosurgery
Picture naming
Connectivity
Plasticity

ABSTRACT

The dynamic connectome perspective states that brain functions arise from the functional integration of distributed and/or partly overlapping networks. Diffuse low-grade gliomas (DLGG) have a slow infiltrating character. Here we addressed whether and how anatomical disconnection following DLGG growth and resection might interfere with functional resting-state connectivity, specifically in relation to picture naming.

Thirty-nine native French persons with a left DLGG were included. All underwent awake surgical resection of the tumor using direct brain electrostimulation to preserve critical eloquent regions. The anatomical disconnectivity risk following the DLGG volume and the resection, and the functional connectivity of resting-state fMRI images in relation to picture naming were evaluated prior to and three months after surgery. Resting-state connectivity patterns were compared with nineteen healthy controls.

It was demonstrated that picture naming was strongly dependent on the semantic network that emerged from the integration and interaction of regions within multiple resting-state brain networks, in which their specific role could be explained in the light of the broader resting-state network they take part in. It emphasized the importance of a whole brain approach with specific clinical data input, during resting-state analysis in case of lesion. Adaptive plasticity was found in secondary regions, functionally connected to regions close to the tumor and/or cavity, marked by an increased connectivity of the right and left inferior parietal lobule with the left inferior temporal gyrus. In addition, an important role was identified for the superior parietal lobe, connected with the frontal operculum, suggesting functional compensation by means of attentional resources in order to name a picture via recruitment of the frontoparietal attention network.

Glossary

DES:	direct electric stimulation
DLGG:	diffuse low grade glioma
DMN:	default mode network (d = dorsal, v = ventral).
DM-PFC:	dorsal medial prefrontal gyrus
ECN:	executive control network
FDR:	false discovery rate
IFG:	inferior frontal gyrus
ITG:	inferior temporal gyrus
IPL:	inferior parietal lobule
MFG:	middle frontal gyrus
MTG:	middle temporal gyrus
ROI:	region of interest
SFG:	superior frontal gyrus
SM1:	primary sensorimotor cortex
SMA:	supplementary motor area
SPL:	superior parietal lobule
STG:	superior temporal gyrus
TAcq:	time of acquisition

* Corresponding author at: I2FH, Institut d'imagerie Fonctionelle Humaine, Montpellier University Hospital, Gui de Chauliac, 80 av. Augustin Fliche, 34295 Montpellier, France.
E-mail address: l-vandokkum@chu-montpellier.fr (L.E.H. van Dokkum).

https://doi.org/10.1016/j.nicl.2019.102010
Received 1 October 2018; Received in revised form 9 September 2019; Accepted 17 September 2019
Available online 24 October 2019

TE: time of echo
TR: Time of repetition
VM-PFC: ventral medial prefrontal gyrus
WSRT: wilcoxon matched pair signed rank test

1. Introduction

Diffuse low-grade gliomas (DLGGs) represent a specific type of invasive brain tumors that migrate along white matter pathways. DLGGs have the particularity of showing limited clinical signs despite their size and location, at least until malignant transformation (Duffau and Taillandier, 2015). This is explained by their slowly infiltrating character that allows for progressive plasticity, i.e. brain reorganization in order to optimize functioning, as the tumor grows (Duffau, 2014). Exhaustive neurological examination is however able to show subtle changes in neurocognitive functioning (Duffau, 2013) that cannot be explained by tumor location alone (Taphoorn and Klein, 2004).

Based on its non-invasive character, resting-state fMRI is currently of high interest for its potential in presurgical mapping of eloquent regions, especially when patients are unable to cooperate with the task fMRI requirements. Regions that show correlated spontaneous fluctuations at rest are defined as resting-state networks. Resting-state analysis in relation to tumor growth demonstrated widespread changes in network strength and organization that were correlated to changes in psychomotor functioning, working memory, attention and information processing (Bosma et al., 2009).

Language is a complex cognitive function that involves multiple processing levels and mechanisms, sub serving efficient human communication that goes far beyond "understanding what is said and saying what is thought" (Tzourio-Mazoyer et al., 2004). Picture naming is a well-known speech-language task that requires visual perception/recognition and lexical access that encompasses the retrieval of both the semantic features and the phonological form of the target word (Baldo et al., 2013). Identified critical regions for picture naming include the left posterior superior temporal gyrus/inferior parietal lobule, posterior middle and inferior temporal gyrus and underlying white matter, and posterior mid-inferior frontal gyrus (Tate et al., 2014; Baldo et al., 2013; Herbet et al., 2016), forming functional networks of cortical structures interconnected by white matter fascicles. Within these networks, cortical lesions as well as the amount of white matter tract disruption have been related to lasting functional deficits (Almairac et al., 2015; Herbet et al., 2015; Thiebaut de Schotten et al., 2014).

Here we addressed the important question whether and how resting-state connectivity changes over time, in relation to anatomical disconnectivity resulting from both the tumor volume before surgery and the subsequent resection (with eventual tumor residual), and subsequently, how the eventual changes impact picture naming. In line with the connectome framework, in which function results from the integration and potentiation of parallel and even sometimes overlapping sub-circuits (Duffau, 2017), we use a whole brain approach to evaluate the functional connectivity of 14 different pre-defined resting-state networks including language and non-language processing related networks (Shirer et al., 2012). We compared resting-state networks before and after surgery with healthy controls, focusing on (a) functional connectivity, (b) anatomical disconnectivity and (c) in relation to picture naming. Firstly, we expected that the anatomical disconnectivity induced by the tumor would impact functional connectivity of resting-state networks before surgery. Secondly, we expected that the DLGG resection would induce additional modifications, allowing restoration of 'healthy' connectivity profiles and/or inducing secondary functional adaptations, like the potential recruitment of regions in the contralesional hemisphere (Vilasboas et al., 2017).

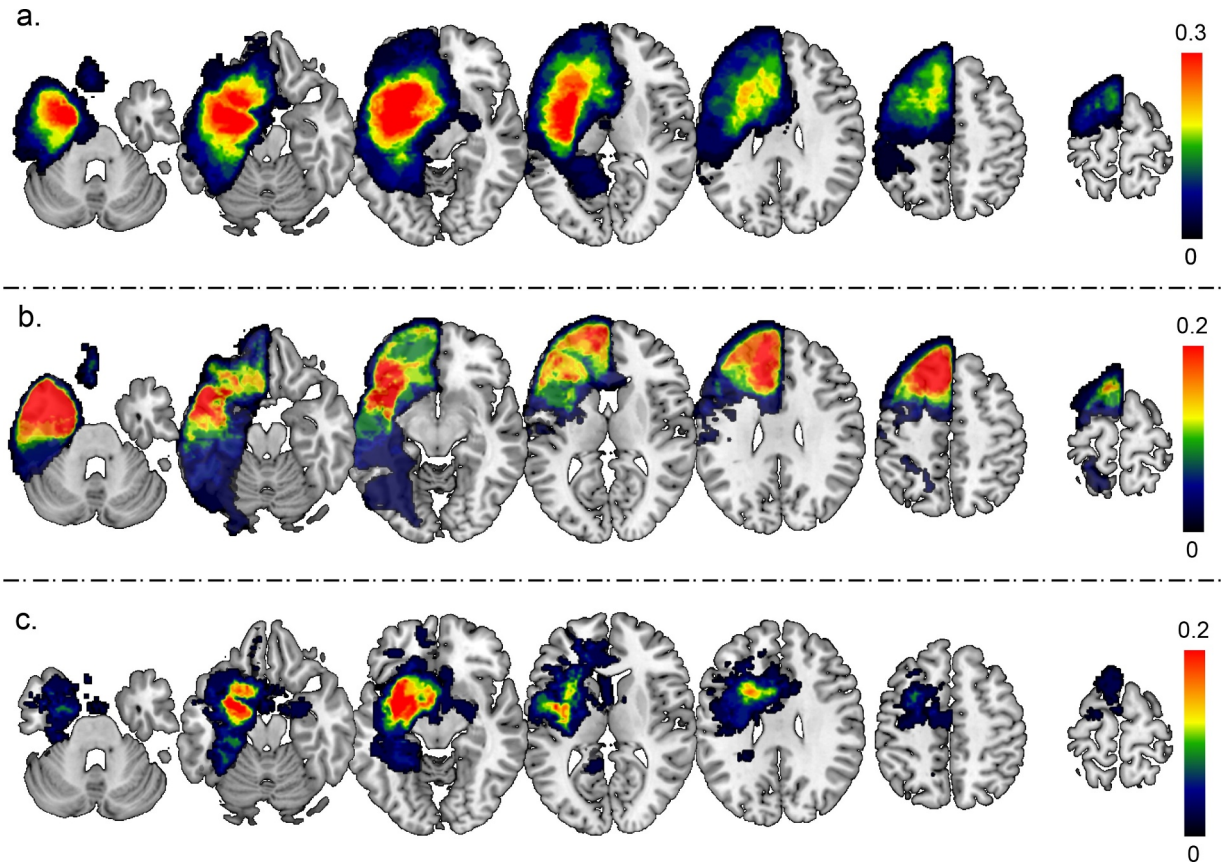

Fig. 1. DLGG location density plot, with (a) Sum of DLGG masks pre-surgery, (b) sum of DLGG masks resection and (c) sum of DLGG masks residue. Each voxel's alue corresponds to the number of tumors in the specific location.

2. Material and methods

2.1. Participants

Thirty-nine French native speakers (17 male, 38.6 ± 8.3 years, 13.85 ± 2.79 years of education, 31 right-handed) were included between 2012 and 2015. All were diagnosed with a left diffuse low-grade glioma (DLGG) in language related regions (n,%: 8, 20.5% temporal; 18, 46.2% frontal; 9, 23.1% frontotemporal; 3, 7.7% parietal; and 1, 2.6% insular) and indicated for awake surgery for the first time. Standard neurological examination was performed to exclude participants that suffered from other neurological or psychiatric disorders. Superimposed DLGG locations before surgery and resection area plus DLGG residue are shown in Fig. 1.

Awake surgery was performed under local anesthesia, using cortico-subcortical mapping by direct electrostimulation (DES) to maximize the extent of tumor resection while preserving the integrity of functional structures. Standard surgery procedures were performed by a well-experienced neurosurgeon (H.D., Duffau et al. 2002, 2005). Prior to and 3 months after surgery, functional MRI resting-state images and picture naming scores were collected. Picture naming was evaluated by a senior speech-language therapist (S.M.G.). All participants benefited from systematic post-operative speech-language therapy during the three months post-surgery (three to five sessions per week).

Patients imaging data was compared with that of 19 healthy controls (12 male, 42.4 ± 12.1 years; 13.0 ± 3.11 years of education, 18 right-handed), with no history of neurological, psychiatric or orthopedic disease, and that was comparable to the patient group in age ($p = 0.18$), years of education ($p = 0.31$) and gender ($p = 0.41$). Additional MRI costs and administrational load obliged us to adapt a 2:1 control - patients design, reflecting the trade-off between costs and minimal scientific requirements. All participants gave informed consent before inclusion. Procedures were compliant with the declaration of Helsinki and approved by the local ethical committee.

The study was part of a larger protocol, including task-based functional MRI analysis of picture naming and its plasticity, whereby participants performed the picture naming task within the scanner in a covert manner. Results are reported separately (Deverdun et al., 2019).

2.2. Picture naming

Participants performed a picture naming task outside of the scanner. The test consists of overtly naming 80 black and white images representing various living and manufactured semantic categories (DO80, Metz-Lutz et al., 1991). Both categories include a comparable number of high and low frequency words, as well as an equal representation of 1 to 4 syllable words. All images are to be found in the Snodgrass and Vanderwart picture database (1980).

2.3. Procedures

During the acquisition of the functional MRI resting-state images, participants were instructed to lay still and not think of anything in particular. Patient images were collected on a 3T whole body magnet (Skyra, Siemens, Germany) with 32 channels head coil. Control participants were scanned once. An axial contrast-enhanced 3D gradient-echo T1-weighted sequence (TE = 2.54 ms, TR = 1690 ms, flip angle = 9°, voxel size = $0.98 \times 0.98 \times 1$ mm^3, 176 slices) was obtained for each participant. Tumor location was precisely defined using a sagittal 3D Fluid-Attenuated Inversion Recovery (FLAIR) image (TE = 384 ms, TR = 5000 ms, Time of Inversion = 1800 ms, voxel size = $0.9 \times 0.9 \times 1.2$ mm^3, 160 slices, TAcq = 4 min 57). A field map was acquired by means of a gradient echo-echo planar imaging sequence (GE-EPI) (TE = 738 ms, TR 436 ms, flip angle = 60°, voxel size = $2.56 \times 2.56 \times 3$ mm^3, 39 slices). Resting-state acquisitions consisted of 200 volumes with the following parameters: TE = 30 ms, TR = 2400 ms, flip angle = 90°, voxel size = $2.4 \times 2.4 \times 3$ mm^3, 39 slices, no interslice gap, TAcq = 8 min 07.

Resting state functional magnetic resonance imaging (fMRI) calculates the functional connectivity at rest based on the spontaneous low-frequency fluctuations of the cerebral blood-flow. These slow fluctuations at rest are thought to reflect interactions that are necessary to maintain the integrity of networks (Fox and Raichle, 2014), whereby those regions whose fluctuations correlated in time are estimated to be part of the same network (Friston et al., 1993).

2.4. Preprocessing

The first five volumes of the resting state acquisitions were discarded to allow for equilibration of the magnetic field as well as patients habituation to the scanning environment. Images were preprocessed using SPM12 (http://www.fil.ion.ucl.ac.uk/spm) in MATLAB (R2012a, The Mathworks). Images were reoriented to the anterior commissure, slice-time corrected, unwrapped, realigned to the first volume, motion corrected, co-registered to the 3DT1, normalized and smoothed (FWHM 6mm filter). Note that normalization of the brain to MNI (Montreal Neurological Institute) stereotactic space is critical in the presence of tumors or resection cavities. Based on experience and previous studies a DARTEL approach was applied without tumor masking (Ripollés et al., 2012). Each normalized image was subsequently reviewed to detect inconsistent deformations.

2.5. Anatomical connectivity

Anatomical connectivity, or rather its disconnectivity was analyzed using the Brain Connectivity Behaviour (BCB) toolkit (http://www.brainconnectivitybehaviour.eu). It provides for a given lesion the probability of each voxel in the brain to be disconnected based on the white matter tracks passing through or emanating from the lesion. The analysis uses a tractography-based atlas of white matter fibers in MNI space (Rojkova et al. 2015). Disconnectome scores (ds) range from 0 (intact connectivity) to 1 (complete disconnectivity). Lesion masks were extracted from tumor and cavity volumes that were manually contoured by an experience neuroradiologist using MRIcron (http://people.cas.sc.edu/rorden/mricron/index.html) and spatially normalized in MNI stereotactic space using the T1 normalization parameters.

Disconnectome scores were subsequently calculated for the predefined resting-state networks, based on the mean value of all voxels within each ROI of each network (Table 1). By means of repeated measures ANOVAs with Greenhouse-Geisser correction for non-sphericity, and Bonferroni correction for main effects we compared (1) disconnectome scores between networks with TIME (pre- and post-surgery) and NETWORK as within factors for global network disconnectivity, and (2) disconnectome scores within each network with TIME and ROI as within factors. Interaction effects were evaluated with the Wilcoxon matched pair Signed Rank Test (WSRT). Picture naming scores were added as covariates to the repeated measures ANOVAs to evaluate the possible linkage between anatomical disconnectivity risk and task performance.

2.6. Functional connectivity

The functional connectivity of the resting-state network ROI that showed a correlation between change in disconnectivity and change in picture naming was evaluated using a seed-to-voxel analysis. The ROI were taken as seed, and the whole-brain was used as target (T-threshold $p < 0.001$, corrected at cluster level $p < 0.05$). Clusters were identified with the AAL toolbox (local maximum analysis, Tzourio-Mazoyer et al., 2002).

Next, functional connectivity within each predefined resting state network was addressed using a ROI-to-ROI connectivity analysis,

Table 1
Overview of resting-state networks and their regions of interest

Network	Region of Interest	Brodmann Area
Dorsal DMN	1) medial prefrontal, anterior cingulate, orbitofrontal cortex; 2) angular gyrus L; 3) superior frontal gyrus R; 4) posterior cingulate cortex, precuneus; 5) midcingulate cortex; 6) angular gyrus R; 7) thalamus L,R; 8) hippocampus L; 9) hippocampus R	1) *9, 10, 24, 32, 11;* 2) *39*; 3) *9*; 4) *23, 30*; 5) *23*; 6) *39*; 7) *N/A*; 8) *20, 36, 30*; 9) *20, 36, 30.*
Ventral DMN	1) retrosplenial, posterior cingulate cortex L; 2) middle frontal gyrus L; 3) parahippocampal gyrus L; 4) middle occipital gyus L; 5) retrosplenial, posterior cingulate cortex R; 6) precuneus; 7) superior, middle frontal gyrus R; 8) parahippocampal gyrus R; 9) angular, middle occipital gyrus R; 10) cerebellum lobule IX R	1) *29, 30, 23*; 2) *8, 6*; 3) *37, 20*; 4) *19, 39*; 5) *30, 23*; 6) *7, 5*; 7) *9, 8*; 8) *37, 30;* 9) *39, 19*; 10) *N/A.*
Language	1) Inferior frontal gyrus; 2) middle temporal gyrus, angular gyrus L; 3) middle, superior temporal, supramarginal, angular gyrus L; 4) inferior frontal gyrus R; 5) supramarginal, superior, middle temporal gyrus R; 6) cerebellum crus I L.	1) *45, 47*; 2) *21, 37, 39*; 3) *21, 22, 42, 40, 39*; 4) *47, 45*; 5) *21, 22, 40*; 6) *N/A.*
LECN	1) middle, superior frontal gyrus L; 2) inferior, orbitofrontal gyrus L; 3) inferior, superior parietal gyrus, precuneus, angular gyrus L; 4) inferior, middle temporal gyrus L; 5) cerebellum crus I R; 6) thalamus L	1) *8, 9*; 2) *45, 47, 10*; 3) *7, 40, 39*; 4) *20, 37;* 5) *N/A*; 6) *N/A.*
RECN	1) middle, superior frontal gyrus R; 2) middle frontal gyrus R; 3) inferior parietal, supramarginal, angular gyrus R; 4) superior frontal gyrus R; 5) cerebellum crus I, crus II, lobule VI L; 6) caudate R	1) *46, 8, 9*; 2) *10, 46*; 3) *24, 32, 8. 6*; 4) *46, 9*; 5) *48, 47*; 6) *N/A*; 7) *N/A.*
Anterior Salience	1) middle frontal gyrus L, 2) insula L; 3) anterior cingulate, medial prefrontal, supplementary motor area; 4) middle frontal gyrus R; 5) insula R; 6) cerebellum lobule VI, crus I L; 7) cerebellum lobule VI, crus I R	1) *9, 46*; 2) *8, 6*; 3) *24, 32, 8, 6*; 4) *46, 9*; 5) *48, 47*; 6) *N/A*; 7) *N/A.*
Posterior Salience	1) middle frontal gyrus L; 2) supramarginal, inferior parietal gyrus L; 3) precuneus L; 4) midcingulale cortex R; 5) superior parietal gyrus, precuneus R; 6) supramarginal, inferior parietal gyrus R; 7) thalamus L; 8) cerebellum lobule VI; 9) posterior insula, putamen L; 10) thalamus R; 11) cerebellum lobule VI; 12) posterior insula R	1) *46*; 2) *40*; 3) *5*; 4) *23*; 5) *7, 5*; 6) *2, 40*; 7) *N/A*; 8) *N/A*; 9) *48*; 10) *N/A*; 11) *N/A*; 12) *48.*
Visuo-spatial	1) middle, superior frontal, precentral gyrus L; 2) inferior parietal sulcus L; 3) frontal operculum,inferior frontal gyrus L; 4) inferior temporal gyrus L; 5) middle frontal gyrus R; 6) inferior parietal lobule R; 7) frontal operculum, inferior frontal gyrus R; 8) middle temporal gyrus R; 9) cerebellum lobule VIII, VIIb L; 10) cerebellum lobule VIII, VIIb R; 11) cerebellum lobule VI, crus I R	1) *6*; 2) *2, 40, 7*; 3) *44, 48, 45*; 4) *37*; 5) *6*; 6) *2, 40, 7*; 7) *44, 48*; 8) *37*; 9) *N/A*; 10) *N/A*; 11) *N/A.*
High visual	1) middle, superior occipital gyrus L; 2) middle, superior occipital gyrus R	1) *18, 19, 17*; 2) *17, 18, 19.*
Primary visual	1) calcarine sulcus; 2) thalamus LR	1) *17*; 2) *N/A*
Basal ganglia	1) thalamus, caudate L; 2) thalamus, caudate, putamen R; 3) inferior frontal gyrus L; 4) inferior frontal gyrus R; 5) pons	1) *N/A*; 2) *N/A*; 3) *45, 48*; 4) *45, 48*; 5) *N/A.*
Precuneus	1) midcingulate, posterior cingulate cortex; 2) precuneus; 3) angular gyrus L; 4) angular gyrus R	1) *23*; 2) *7, 19*; 3) *7, 40*; 4) *7, 40.*
Sensori-motor	1) pre, post central gyrus L; 2) pre, post central gyrus R; 3) supplementary motor area; 4) thalamus L; 5) cerebellum lobule IV, VI, VI bilateral; 6) thalamus R.	1) *4, 2*; 2) *4, 6, 3*; 3) *6*; 4) *N/A*; 5) *N/A*; 6) *N/A.*
Auditory	1) superior temporal, heschl's gyrus L; 2) superior temporal gyrus R; 3) thalamus R	1) *22, 48*; 2) *22, 38, 42, 48*; 3) *N/A.*

evaluating connectivity compared to controls, and within patients over time in relation to change in picture naming performance with the CONN functional connectivity toolbox (16a; https://www.nitrc.org/projects/conn; Whitfield-Gabrieli and Nieto-Castanon, 2012) in Matlab R2102a, including denoising with a band-pass filter [0.008; 0.09] and linear detrending. The significance threshold was set at 0.05 with a two-sided cluster-extended FDR (false discovery rate) correction.

3. Results

3.1. Picture naming

Performance scores were collected for 34/39 participants at both time points. Of those, 16 participants decreased in performance, 11 improved and 7 showed no change after surgery. Overall, participants performed slightly worse on the picture naming test post-surgery (WSRT, $p = =0.038$), with a mean score of 78.9/80 before and 77.4/80 after surgery. Unfortunately, the five patients with missing picture naming data were all left-handed. Any questions about the influence of hemispheric dominance on resting state plasticity in relation to picture naming remained unanswered.

3.2. Anatomical disconnectivity

Recall that the disconnectivity score represents the probability that a certain ROI is anatomically disconnected resulting from the lesion. Disconnectivity scores differed significantly between networks, independent of time (NETWORK: Greenhouse-Geisser $F_{(1,3.5)} = =44.27$, $p < 0.001$, $\eta = =0.573$).

Focusing on the individual ROI within each network it was found (a) that the disconnectivity scores of each individual ROI were highly correlated over time ($p < 0.001$), (b) that the subcortical ROI showed consistent higher risks to be disconnected (>45%), whereas (c) right-hemispheric ROI showed consistent lower disconnectivity risks (<10%).

Within the individual resting-state networks, effects of TIME (interaction as well as main effects) were observed for 8 out of 14 networks. Main effects of time represented a general decrease of the network's disconnectivity. Post-hoc related-sampled WSRT highlighted that especially the disconnectivity scores of the cerebellar ROI and thalami decreased significantly over surgery, whereas increased disconnectivity scores were observed for the left supramarginal and middle/superior temporal gyri.

By adding change in picture naming scores as a covariate to the repeated measures ANOVA, effects of time were maintained in 5 of the networks (posterior salience, primary visual, language, auditory and sensorimotor network), indicating that these specific changes were unrelated to change in task performance: improved connectivity of bilateral cerebellum 4/5/6, and of both thalami as well as a decreased connectivity of the supramarginal, superior and middle temporal gyri post-surgery. Contrarily, in 3 networks the effects of time disappeared when corrected for differences in task-performance (both executive networks and the ventral DMN), highlighting that the changes in disconnectivity scores of the right parahippocampal gyrus, the right and left cerebellum crus 1 and the right and left middle/superior frontal gyri were of importance for picture naming.

Moreover, A Pearson's correlation analysis between change in disconnectivity score and change in picture naming scores highlighted that the disconnectivity of the left superior temporal gyrus (STG, $r = = -0.385$, auditory network), left middle frontal gyrus (MFG, $r = = -0.428$, post-salience network), right superior parietal lobule (SPL, $r = = -0.378$, post-salience network) and right inferior parietal

Table 2
Disconnectivity changes over time for each resting-state network.

	Nn°	Effect REGION[F p η]	Least disconnected ROI (ds)	Most disconnected ROI (ds)	Effects TIME [F p η]	Effects TIME + ΔDO80 [F p η]	Post-hoc WSRT, effect of timep < 0.05
dDMN	9	44.20, 0.00, 0.65	Angular R (0.018)	Thalamus L (0.676)	X	x	X
vDMN	10	20.98, 0.00, 0.43	Angular R (0.063)	Parahippocamp L (0.451)	Main [5.46, 0.00, 0.16]	x	General decrease, Especially for parahippocamp R
Language	7	23.45, 0.00, 0.51	Frontal inf R (0.094)	Temporal mid L (0.420)	Interact [3.52, 0.02, 0.13]	Interact [3.01, 0.04, 0.14]	Increase: Supramarginal, temporal mid/sup L Decrease: cereb crus I L.
LECN	6	30.06, 0.00, 0.49	Parietal inf/angul L (0.198)	Thalamus L (0.721)	Interact [3.09, 0.03, 0.09]	x	Decrease: cereb crus I R, front mid/sup L
RECN	6	18.52, 0.00, 0.43	Parietal inf/angul R (0.047)	Caudate R (0.517)	Interact [3.19, 0.03, 0.11]	X	Decrease: cereb crus I/II L + vermis, caudate R, front mid/sup R
Salience	7	7.569, 0.00, 0.22	Insula R (0.088)	Cingulate ant (0.337)	x	X	x
Post-Salience	12	93.99, 0.00, 0.81	Supramarginal R (0.045)	Thalamus L (0.846)	Main [12.29, 0.00, 0.33] Interact [3.73, 0.01, 0.13]	Main [8.25, 0.01, 0.28]	General decrease, especially for cereb VI L, thalamus R
Visuo-spatial	11	15.59, 0.00, 0.42	Temporal inf/mid R (0.041)	Frontal inf/oper L (0.343)	x	x	x
High-visual	2	42.87, 0.00, 0.57	Occipital mid/sup R (0.066)	Occip mid/sup L (0.196)	x	x	x
Primary visual	1	x	Calcerine/occip inf RL (0.117)	x	Main [6.85, 0.01, 0.18]	Main [5.54, 0.03, 0.17]	General decrease, especially for Thalamus L
Basal ganglia	5	24.33, 0.00, 0.54	Frontal inf R (0.294)	Thalamus L (0.869)	x	x	x
Precuneus	4	88.28, 0.00, 0.76	Angular R (0.038)	Cingul mid/post RL (0.445)	x	x	x
Sensori-motor	6	64.72, 0.00, 0.68	Central pre/post R (0.117)	Thalamus L (0.837)	Main [9.76, 0.00, 0.25]	Main [6.73, 0.02, 0.21]	Decrease: Cereb IV-VI + vermis B, thalamus B, SM1 B, SMA B.
Auditory	3	51.69, 0.00, 0.70	Temporal sup R (0.063)	Thalamus R (0.532)	Main [11.72, 0.00, 0.27] Interact [6.25, 0.01, 0.17]	Main [7.16, 0.01, 0.21]	General decrease, especially for thalamus R

Nn = number of regions within network, ROI = region of interest, ds = disconnectome score. η = partial eta squared. +ΔDO80 = change in score on the DO80 picture naming task, added as a covariate to the ANOVA, WSRT = post-hoc Wilcoxon Signed Rank Test pre-post surgery.

Table 3
The functional connectivity of those regions whose disconnectivity was related to picture naming

SEED	Functionally connected region	T	p-cluster	k	[x,y,z]
Parietal inf R	Temporal inf L	5.05	0.005	30	[-48 -18 -36]
Parietal sup R	Calcerine R	5.44	0.001	49	[22 -66 04]
	Precuneus R	5.02	0.005	30	[12 -66 30]
	Insula R	4.16	0.009	26	[36 20 06]
Temporal sup L	No functional connectivity				
Frontal mid L	Parahippocamp L	4.99	0.038	15	[-12 -04 -36]

Seed-to-voxel analysis. Connected regions were defined with a T-threshold < 0.001, p-cluster < 0.05, and cluster-size (k) > 10. Stronger connectivity post-surgery is related to better picture naming performance. R = right, L = left, [x,y,z] = cluster coordinates in MNI space.

lobule (IPL, $r = = -0.369$, visuospatial network) were significantly ($p < 0.05$) related to task performance, whereby increased disconnectivity scores were linked to decreased picture naming scores, i.e. a worse task-performance. An overview of these results can be found in Table 2.

3.3. Functional connectivity

As described above, four ROI showed a direct correlation between change in disconnectivity scores and change in picture naming: The right IPL, right SPL, left STG and left MFG. Via a seed-to-voxel analysis the functional connectivity of these seed ROI was evaluated. In Table 3 an overview of results can be found, whereby a stronger functional connectivity post-surgery is related to a better picture naming score. A repeated analysis incorporating the change in disconnectivity confirmed the results, indicating that they highlight indeed functional plasticity rather than modified anatomical connectivity.

Next, functional connectivity within each predefined resting state network was addressed using a ROI-to-ROI connectivity analysis, evaluating connectivity (a) compared to controls, and (b) within patients in relation to change in picture naming performance.

Compared to controls, it was found that several resting-state networks showed comparable connectivity patterns before and after surgery, i.e. the basal ganglia, the precuneus, the auditory and executive functioning networks. The functional connectivity of these networks seemed unaltered by either the tumor volume or the resection of the tumor. In contrast, we found networks that showed plasticity before surgery, i.e. the language, sensori-motor, vDMN and visual networks, and networks that showed plasticity after surgery, i.e. the dDMN, salience, and post-salience network, but not with the tumor. And, finally there was one network that showed plasticity before as well as after surgery, i.e. the visuospatial network.

Within patients, only three of the above mentioned networks showed changes in functional connectivity that were correlated with picture naming performance: the dDMN, the vDMN and the visuospatial network. That is, task performance improved post-surgery when there was: (1) a less strong connectivity between the left medial prefrontal cortex (including the anterior cingulate gyrus) and the left hippocampus in the dDMN, (2) a stronger connectivity between the posterior cingulate gyrus and the right middle and superior frontal gyrus within in the vDMN, and (3) a stronger connectivity of the left inferior temporal gyrus with both the left inferior parietal sulcus and the cerebellar lobules 7b/8 in the visuospatial network. See Table 4 for an overview of changes in functional connectivity within the resting-state networks.

4. Discussion

First and foremost, it is worth recalling that (1) this study dealt with patients presenting a DLGG, known to induce major functional

Table 4
Overview of resting-state network functional connectivity changes compared to controls and within patients in relation to language task performance over time.

	Network	+/-	Altered functional connectivity	T, p-FDR
Pre (vs. controls)				
	Language	⇓	Middle temporal gyrus L → superior temporal/inferior parietal L	−2.70, 0.046
	Sensorimotor	⇑	Cerebellum 4/5/6 + vermis B → pre/post central gyrus L	2.83, 0.032
	vDMN	⇓	Middle frontal gyrus L → parahippocampal gyrus L	−2.99, 0.038
	Visual	⇑	Thalamus L → middle/superior occipital gyrus R	2.48, 0.048
Post (vs. controls)				
	dDMN	⇑	Inferior parietal (angular) gyrus R → superior frontal gyrus R	2.86, 0.037
		⇓	Inferior parietal (angular) gyrus L ←→ middle cingulated gyrus	−2.88, 0.047
	Salience	⇓	Insula R → Insula L	−2.73, 0.043
	Post Salience	⇑	Posterior insula L → superior parietal gyrus/precuneus R	3.38, 0.015
Pre and Post (vs. controls)				
	Visuospatial	⇑	Inferior parietal gyrus R → inferior parietal gyrus L	3.16, 0.025
Improved task performance (within patients)				
	vDMN	⇑	Posterior cingulate cortex ←→ middle/superior frontal gyrus R	3.51, 0.013
	dDMN	⇓	Anterior cingulate cortex / medial prefrontal gyrus L → hippocampus L	−3.51, 0.011
	Visuospatial	⇑	Inferior temporal gyrus L → inferior parietal gyrus L	3.13, 0.038
		⇑	Inferior temporal gyrus L → cerebellum 7b/8 R	2.82, 0.041

Pre = pre-surgery, post = post-surgery, ⇑ = increased and ⇓ = decreased functional resting-state connectivity compared to controls or within patients, R = right, L = left, B = bilateral. Corrected at FDR-seed level, two-sided, $p < 0.05$.

plasticity phenomena (Bonnetblanc et al., 2006), (2) all patients underwent awake surgery with direct electrostimulation, hence it can be assumed that critical eloquent regions have been preserved (Duffau, 2013) and (3) all patients had three months of intensive speech-language therapy following surgery. In this context, we had the unique opportunity to evaluate changes in resting-state connectivity before and after surgery within the patient population compared to that of healthy controls. In addition, we were able to confront these changes with changes in performance on a picture naming task.

The tumor resection decreased the average anatomical disconnectivity score of each resting-state network, suggesting that the DLGG itself has a disruptive impact on brain functioning (Bosma et al., 2009; Derks et al., 2017). Evidently, those ROI that were situated in the principal tumoral frontotemporal areas, showed increased disconnectivity after resection. In addition, the functional connectivity strength between temporal ROI was decreased compared to controls. Based on the important implication of the left temporal lobe in language processing, and more specifically of the middle temporal lobe for picture naming, it was expected that all of these changes would be related to worse task performances (Baldo et al., 2013). This was, however, not the case. These findings actually highlight the impact of adaptive plasticity. As plasticity presumably occurred before surgery, the increased disconnectivity post-surgery did not influence picture naming scores any more than the tumor already did.

4.1. Observed adaptive plasticity

So, how can we explain changes in picture naming performance post-surgery? Which adaptive connections and/or supportive regions might play an essential role in maintaining performance levels, if the eloquent regions cannot explain the level of performance? Starting with the adaptive plasticity before surgery, changes were observed within the sensorimotor, the visual, the vDMN, and the visuospatial network, the latter two being related to picture naming. That is, compared to controls, patients showed a) a stronger input from the right to the left IPL, b) a stronger connection between the cingulate gyrus (posterior part) and the right MFG/SFG, and c) better picture naming scores were related to an increased connectivity of the left ITG with both the left IPL and the right cerebellum.

Next, the decreased anatomical disconnectivity score of four ROI (i.e. the increased anatomical connectivity after surgery) was also correlated with better picture naming: the left MFG and right SPL of the post-salience network, the right IPL of the visuospatial network and the left STG of the auditory network. The subsequent functional connectivity analysis in relation to task performance highlighted that (a) the right IPL was functionally connected to the left ITG, (b) the left MFG was functionally connected to the left parahippocampal gyrus, (c) the right SPL was functionally connected to the right calcerine, frontal operculum and precuneus and (d) the left STG was not functionally connected to any other ROI.

The left STG relates primarily to speech perception and phonological processing rather than to retrieval of word meaning (Indefrey and Levelt, 2004). Activation of the left STG during picture naming is associated with self-monitoring (auditory feedback) of spoken words (Abel et al., 2009). This might directly explain why we did not find any functional connectivity of the left STG in relation to the task (Fig. 2a): picture naming was indeed performed overtly only outside of the scanner not during the acquisition of resting-state MRI. Auditory feedback was then not solicited in the scanner.

4.2. The crucial role of the semantic network

A large meta-analysis, including 120 functional neuroimaging studies that addressed semantic processing by giving meaning to words (spoken or written), highlighted a distinct left-lateralized network consisting of 7 regions: (1) the posterior inferior parietal lobule (the angular gyrus with portions of the supramarginal gyrus), (2) the lateral temporal cortex (the middle and portions of the inferior temporal gyrus), (3) the fusiform and parahippocampal gyri, (4) the dorsomedial prefrontal cortex, (5) the inferior frontal gyrus, (6) the ventromedial prefrontal cortex and (7) the posterior cingulate gyrus (Binder et al., 2009). In the present study, when combining the findings of the seed-to-voxel and ROI-to-ROI functional connectivity analysis in relation to picture naming, an interesting overlap with this semantic network was observed (Fig. 2). Five out of these seven regions were indeed related to better picture naming performance post-surgery: the left IPL, the left ITG, the left MFG (part of the DM-PFC), the left parahippocampal gyrus and the posterior cingulate gyrus. However, we did not observe any activation of left MTG, IFG and VM-PFC regions. Equally, our network was more bilaterally distributed, and we found an additional activation of the right SPL and the right IPL.

The functions of these various regions within the context of semantics have been well described in the literature. The left IPL, in close connection with the posterior left MTG, is involved in semantic retrieval (Tune and Asaridou, 2016). The left mid-to-posterior ITG with the underlying left inferior longitudinal fasciculus is critical for lexical retrieval (Herbet et al., 2016). The parahippocampal gyrus has been associated with scene recognition (Aguirre et al., 1996), visual memory

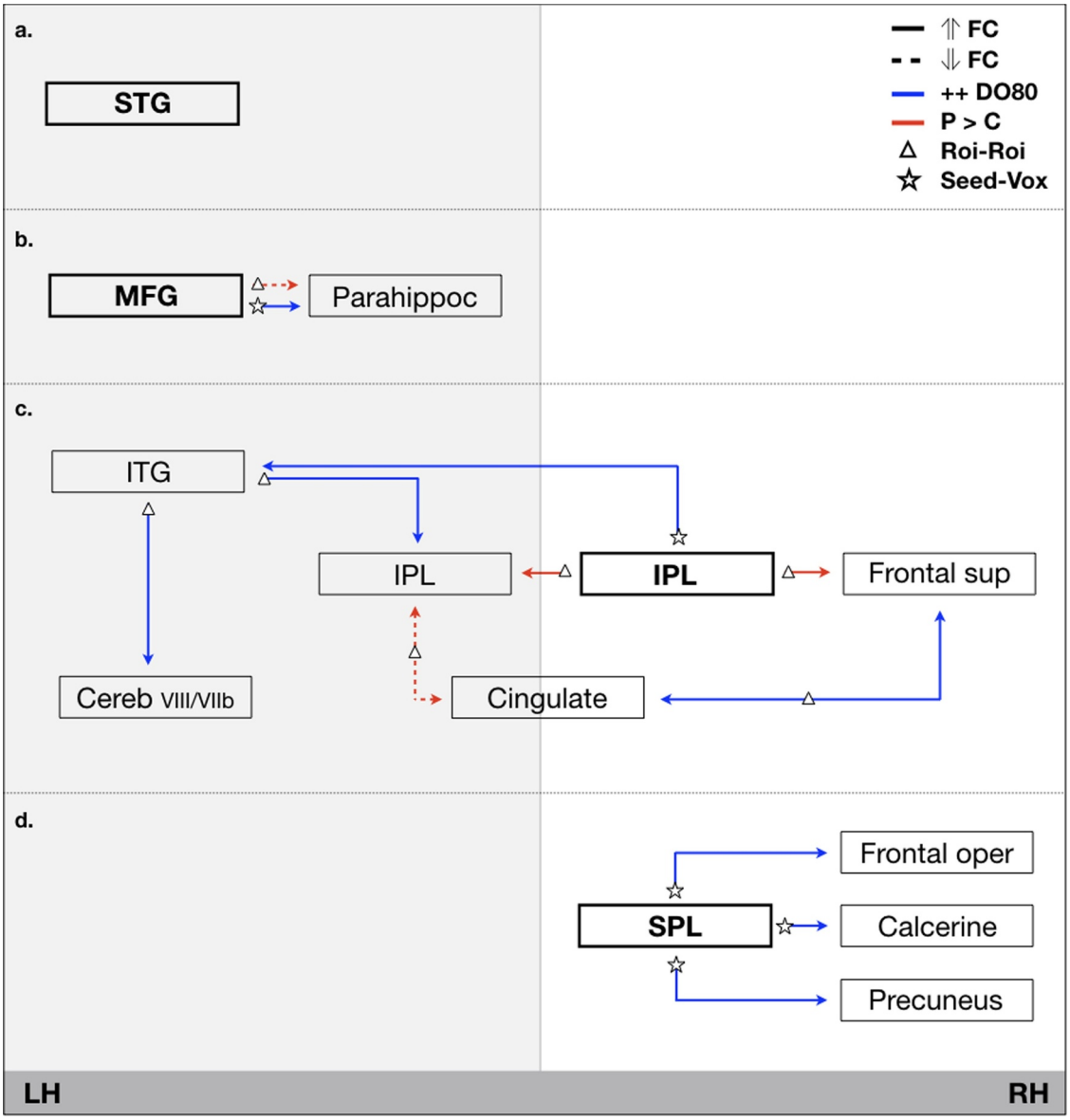

Fig. 2. Schematic representation of main functional connectivity (FC) patterns based on the four key-nodes that showed altered connectivity in relation to better picture naming (+ + DO80) performance post-surgery (blue connections) as well as those that are different to controls (red connections). STG = superior temporal gyrus, ITG = inferior temporal gyrus. IPL = inferior parietal lobule. MFG = middle fonrtal gyrus, SPG = superior parietal lobule, ⇑ = increased (solid line), ⇓ = decreased (dotted line) connectivity, P = patients, C = Controls, LH = left-hemisphere, RH = right-hemisphere. Fig. 2a: altered connectivity of the STG. Fig. 2b: altered connectivity of the left MFG. Fig. 2c: altered connectivity of the network involving the right IPL. Fig. 2d: altered connectivity of the right SPL. (For interpretation of the references to color in this figure legend, the reader is referred to the web version of this article.)

(Stern et al., 1996) and to naming (Wilson et al., 2015). And in connection with the left MFG it is related to the visual recognition of attributes during picture naming of different object categories (Humphreys and Forde, 2001). The strength of this connection post-surgery has been related to better picture naming (current work, Fig. 2b).

4.3. Recruitment of the right hemisphere: the role of directed attention?

As expected, we observed recruitment of regions in the contralesional hemisphere, especially of the right IPL (Fig. 2c) and the right SPL (Fig. 2d). The right IPL was stronger connected to the left IPL in patients compared to controls and the stronger its direct connection with the left ITG, the better was the picture naming performance post-surgery. First, it is well described that the left mid-to-posterior ITG with the underlying left inferior longitudinal fasciculus is critical for lexical retrieval (Herbet et al., 2016), and that the posterior part of the left IPL (angular gyrus) in close relation to the posterior left MTG is involved in semantic retrieval (Tune and Asaridou, 2016). Our results show how the right IPL is connected with both structures post-surgery. Here, the right IPL is identified as being part of the visuospatial network that is composed of mainly frontal, parietal and several temporal regions. This network actually shows strong overlap with the frontoparietal network that is also known as the dorsal attention network, involved in directing visual attention (Corbetta, 1998, Spadone et al., 2015). Interestingly, the second identified right-hemispheric region, the right SPL, is also part of this dorsal attention network (Spadone et al., 2015), whereas in Greicius network definition it is part of the post-salience network. This network is known to be involved in the orientation of attention to the most relevant ongoing event; it shifts attention between internal and external stimuli (Bressler and Menon, 2010). Lesions of the right, but not the left, SPL showed a critical implication in working memory

involving visuospatial manipulation (Koenigs et al., 2009). It has been shown active during both saccadic and attention tasks, highlighting the tight link between attention and eye-movements, supporting intended looking (Simon et al., 2002). Functionally, we found that the right SPL was connected to the right calcerine (visual network), the frontal operculum (part of the frontoparietal network) and the precuneus (part of the DMN network and post-salience).

The stronger link between right sided attentional related regions and the left ITG, critical in lexical retrieval, might indicate that patients had to allocate more attentional resources than healthy controls to perform the picture naming task. Linguistics and cognitive psychology bring us valuable insights in this regard: naming requires the extraction of both the semantic features and the phonological form of the target word, which are controlled by more general cognitive functions such as executive and attentional resources. The link between cognitive functions and language processing has been particularly highlighted in the context of aphasia rehabilitation, in which cognitive status seems to be a key predictor of rehabilitation outcomes (Lambon Ralph et al., 2010; van de Sandt-Koenderman et al., 2012). We may then hypothesize that the more the left hemispheric picture naming network is weakened, the more the right attentional network will be recruited. It would be interesting to study to what extent this over-recruitment of attentional resources may compensate naming difficulties: is the amount of right frontoparietal compensation proportionate to the extent or the location of the left-sided resection, and is there a cut-off point at which this compensation will become insufficient? Also, the amount of attentional resources used might be related to task reaction times and perceived handicap, independent of the actual performance scores that are still at the upper bound of the scale (77.7/80 in this study). It has to be noted, however, that all patients received intensive speech-language rehabilitation during the 3 months post-surgery, which might have trained and strengthened attentional resources.

4.4. Limitations

A question that remained unaddressed in this work is the relationship between the location of the resection, the pattern of connectivity change and its relationship to picture naming. This question is important as it might reveal whether the observed compensation of the frontoparietal network reflects a general compensation strategy, or is only used in specific cases. The current patient group was composed of three principal subgroups: those with a resected frontal, a temporal, and a frontotemporal DLGG. Unfortunately the analysis subgroup remained inconclusive due to the small sample sizes of the latter two groups, being only half the size of the frontal DLGG subgroup. With a sample size below ten participants, individual variations become very important, especially for higher-order functional networks. Thus shared patterns did not meet the threshold for repeated comparisons. A larger effective is required to fully address this question. Nevertheless, previously we have shown that restingstate connectivity between homotopic regions was generally disturbed independent of the resection area (Coget et al., 2018) and task-based fMRI analysis showed that the functional plasticity during picture naming could not be explained by tumor location and volume (Deverdun et al., 2019). In both cases, the importance of pre-surgical plasticity has been highlighted as well as surgery procedures allowing the preservation of eloquent areas. This seems to coincide with the current observation that tumor resection induced a decrease in the overall average anatomical disconnectivity score of each resting state network. Together this may suggest that tumor growth and resection, independent of its exact location, have a disruptive impact on overall brain functioning, requiring compensational attentional resources.

This work shows an overrepresentation of right-handed patients and, following matching procedures, of healthy controls. Interestingly, the few left-handed participants showed lacking picture naming data. One might wonder whether this is an unfortunate coincidence or related to actual pathology - an interesting question that asks for further investigation with a larger population and the scientific preferable 1:1 patient - control design.

5. Conclusions

We were able to identify the most relevant ROI within the semantic network by confronting resting-state connectivity with performance scores on a task administered outside of the scanner. It seems promising and interesting that we did so without using functional task imaging that requires the execution of a semantic task within the scanner. Starting with pre-defined resting-state networks encompassing the whole brain allowed us to highlight how the language process required for picture naming is dependent on various resting-state networks working together. Id est., we showed how semantic processing results from the integration and interaction of multiple resting-state brain networks, in which the specific semantic role of each region can be explained in the light of the broader resting-state network it takes part in. Or, as Bressler and Menon (2010) framed nicely, we contributed to show how *"Cognitive functions arise from interactions within and between distributed brain systems"*.

It seemed that not the anatomical connectivity or disconnectivity of traditional eloquent regions for semantics were crucial for a better to good task-performance post-surgery, but rather their functional connectivity with secondary supportive regions and/or networks. The decreased connectivity of the MTG with the STG and IPL within the language network was suggested to be compensated by an increased input from the right IPL towards the left IPL, which are both connected to the left ITG and communicate with frontal and cerebellar structures (Fig. 2a). Subsequently, post-surgery a decreased connectivity between the left MFG and the left parahippocampal gyrus was observed compared to controls. However, the stronger this connection within patients, the better was patients scored on picture naming (Fig. 2b).

Lost capacity seemed to be compensated by an increased role of right hemispheric parietal structures including the IPL and the SPL, both being part of the functional frontoparietal attentional network, independently of their individual respective restingstate networks (i.e. the visuospatial and post-salience network). This might implicate that patients post-surgery use attentional resources to compensate for lost function. It also confirms the contribution of the right-hemisphere in language processing, especially in case of DLGG, as described by Vilasboas et al. (2017).

Finally, two general take-home messages could be extracted from this work. First, in case of brain lesion, the traditional approach of focusing on one simple network of interest (e.g. the language network) might not be sufficient to understand adaptive plasticity. A whole brain connectome approach, even though being more complex, seems the best way forward. Second, if one is interested in a specific function of the brain, having clinical input concerning the subject of interest seems imperative to make sense out of resting-state connectivity.

Declaration of Competing Interest

None.

Acknowledgments

This work was supported by LabEx NUMEV (n° AN-10-LABX-20) and an internal funding by the CHU of Montpellier (AOI n° 2010-A01313-36).

References

Abel, S, Dressel, K, Kummerer, D, et al., 2009. Correct and errorneous picture naming responses in healthy subjects. Neurosci. Lett. 463, 167–171. https://doi.org/10.1016/j.neulet.2009.07.077.

Aguirre, GK, Detre, JA, Alsop, DC, D'Esposito, M, 1996. The parahippocampus subserves topographical learning in man. Cereb. Cortex 6, 823–829.
Almairac, F, Herbet, G, Moritz-Gasser, S, de Champfleur, NM, Duffau, H, 2015. The left inferior fronto-occipital fasciculus subserves language semantics: a multilevel lesion study. Brain Struct. Funct. 220, 1983–1995. https://doi.org/10.1007/s00429-014-0773-1.
Baldo, JV, Arevalo, A, Patterson, JP, Dronker, NF, 2013. Grey and white matter correlates of picture naming: evidence from a voxel-based lesion analysis of the Boston naming test. Cortex 49, 658–667. https://doi.org/10.1016/j.cortex.2012.03.001.
Binder, JR, Desai, RH, Graves, WW, Conant, LL, 2009. Where is the semantic system? A critical review and meta-analysis of 120 functional neuroimaging studies. Cereb. Cortex 19, 2767–2796. https://doi.org/10.1093/cercor/bhp055.
Bonnetblanc, F, Desmurget, M, Duffau, H, 2006. Low grade gliomas and cerebral plasticity: fundamental and clinical implications. Med. Sci. 22, 389–394.
Bosma, I, Reijneveld, JC, Klein, M, et al., 2009. Disturbed functional brain networks and neurocognitive function in low-grade glioma patients: a graph theoretical analysis of resting-state MEG. Nonlinear Biomed. Phys. 23, 9. https://doi.org/10.1186/1753-4631-3-9.
Bressler, SL, Menon, V, 2010. Large-scale brain networks in cognition: emerging methods and principles. Trends Cognit. Sci. 14, 277–290. https://doi.org/10.1016/j.tics.2010.04.004.
Coget, A, Deverdun, J, Bonafe, A, van Dokkum, LEH, Duffau, H, Molino, F, Le Bars, E, de Champfleur, NM, 2018. Transient immediate postoperative homotopic functional disconnectivity in low-grade glioma patients. Neuroimage Clin. 18, 656–662. https://doi.org/10.1016/j.nicl.2018.02.03.
Corbetta, M, 1998. Frontoparietal cortical networks for directing attention and the eye to visual locations: identical, independent, or overlapping neural systems? Proc. Natl. Acad. Sci. USA 95, 831–838. https://doi.org/10.1073/pnas.95.3.831.
Derks, J, Dirkson, AR, de Witt Hamer, PC, van Geest, Q, Hulst, HE, Barkhof, F, Pouwels, PJ, Geurts, JJ, Reijneveld, JC, Douw, L, 2017. Connectomic profile and clinical phenotype in newly diagnosed glioma patients. Neuroimage Clin. 16, 87–96. https://doi.org/10.1016/j.nicl.2017.01.007.
Deverdun, J, van Dokkum, LEH, le Bars, E, Herbet, G, Mura, T, D'agata, B, Picot, MC, Menjot, N, Molino, F, Duffau, H, Moritz Gasser, S, 2019. Evidence of functional connectivity changes after resection of low grade gliomas: an fMRI task based connectivity study. Brain Imaging Behav. https://doi.org/10.1007/s11682-019-00114-7. Epub ahead of print.
Duffau, H, 2013. A new philosophy in surgery for diffuse low-grade glioma (DLGG): Oncological and functional outcomes. Neurochirurgie 59, 2–8. https://doi.org/10.1016/j.neuchi.2012.11.001.
Duffau, H, 2014. Diffuse low-grade gliomas and neuroplasticity. Diagn. Interv. Imaging 95, 945–955.
Duffau, H, 2017. The error of Broca: from the traditional localizationist concept to a connectomal anatomy of human brain. J. Chem. Neuroanat. https://doi.org/10.1016/j.jchemneu.2017.04.003.
Duffau, H, Capelle, L, Sichez, N, et al., 2002. Intraoperative mapping of the subcortical language pathways using direct stimulations. An anatomo-functional study. Brain 125, 199–214.
Duffau, H, Gatignol, P, Mandonnet, E, et al., 2005. New insights into the anatomo-functional connectivity of the semantic system: a study using cortico-subcortical electrostimulations. Brain 128, 797–810.
Duffau, H, Taillandier, L, 2015. New concepts in the management of diffuse low-grade glioma: proposal of a multistage and individualized therapeutic approach. Neuro Oncol. 17, 332–342. https://doi.org/10.1093/neuonc/nou153.
Fox, MD, Raichle, ME, 2014. Spontaneous fluctuations in brain activity observed with functional magnetic resonance imaging. Nat. Rev. Neurosci. 8, 700–711.
Friston, KJ, Frith, CD, Liddle, PF, Frackowiak, RSJ, 1993. Functional connectivity: the principal-component analysis of large (PET) data sets. J. Cereb. Blood Flow Metab. 12, 5–14. https://doi.org/10.1038/jcbfm.1993.4.
Herbet, G, Latorre, JG, Duffau, H, et al., 2015. The role of cerebral disconnection in cognitive recovery after brain damage. Neurology 84, 1390–1391. https://doi.org/10.1212/WNL.0000000000001453.
Herbet, G, Moritz-Gasser, S, Boiseau, M, Duvaux, S, Cocherau, J, Duffau, H, 2016. Converging evidence for a cortico-subcortical network mediating lexical retrieval. Brain 139, 3007–3021. https://doi.org/10.1093/brain/aww220.
Humphreys, GW, Forde, EM, 2001. Hierarchies, similarity and inter-activity in object recognition: 'category specific' neurophysiological deficits. Behav. Brain Sci. 24, 453–509.
Indefrey, P, Levelt, WJM, 2004. The spatial and temporal signatures of word production components. Cognition 92, 101–144. https://doi.org/10.3389/fpsyg.2011.00255.
Koenigs, M, Barbey, AK, Postle, BR, Grafman, J, 2009. Superior parietal cortex is critical for the manipulation of information in working memory. J. Neurosci. 29, 14980–14986. https://doi.org/10.1523/JNEUROSCI.3706-09.2009.
Lambon Ralph, MA, Snell, C, Joanne, K, Fillingham, JK, Conroy, P, Sage, K, 2010. Predicting the outcome of anomia therapy for people with aphasia post CVA: Both language and cognitive status are key predictors. Neuropsy. Rehab. 20, 289–305. https://doi.org/10.1080/09602010903237875.
Metz-Lutz, MN, Kremin, H, Deloche, G, 1991. Standardisation d'un test de dénomination orale: contrôle des effets de l'âge, du sexe et du niveau de scolarité chez les sujets adultes normaux. Rev. Neuropsychol. 1, 73–95.
Ripollés, P, Marco-Pallares, J, de Diego-Balaguer, R, et al., 2012. Analysis of automated methods for spatial normalization of lesioned brains. Neuroimage 60, 1296–1306. https://doi.org/10.1016/j.neuroimage.2012.01.094.
Rojkova, K, Volle, E, Urbanski, M, et al., 2015. Atlasing the frontal lobe connections and their variability due to age and education: a spherical deconvolution tractography study. Brain Struct. Funct. 221, 1751–1766. https://doi.org/10.1007/s00429-015-1001-3.
Shirer, WR, Ryali, S, Rykhlevskaia, E, Menon, V, Greicius, MD, 2012. Decoding subject-driven cognitive states with whole-brain connectivity patterns. Cereb. Cortex 22, 158–165. https://doi.org/10.1093/cercor/bhr099.
Simon, O, Mangin, JF, Cohen, L, le Bihan, D, Dehaene, S, 2002. Topographical layout of hand, eye, calculation, and language-related areas in the human parietal lobe. Neuron 33, 475–487.
Snodgrass, JG, Vanderwart, M, 1980. A standardized set of 260 pictures: norms for name agreement, image agreement, familiarity and visual complexity. J. Exp. Psychol. Hum. Learn. Mem. 6, 174–215.
Spadone, S, Della Penna, S, Sestieri, C, Betti, V, Tosoni, A, Gianni Perrucci, MG, Romani, GL, Corbetta, M, 2015. Dynamic reorganization on human resting-state networks during visuospatial attention. Proc. Natl. Acad. Sci. 112, 8112–8117. https://doi.org/10.1073/pnas.1415439112.
Stern, CE, Corkin, S, Gonzales, RG, Guimaraes, AR, Baker, JR, Jennings, PJ, Carr, CA, Sugiura, RM, Vedantham, V, Rosen, BR, 1996. The hippocampal formation participates in novel picture encoding: evidence from functional magnetic resonance imaging. Proc. Natl. Acad. Sci. USA 93, 8660–8665.
Taphoorn, MJ, Klein, M, 2004. Cognitive deficits in adult patients with brain tumors. Lancet Neurol. 3, 159–168. https://doi.org/10.1016/S1474-4422(04)00680-5.
Tate, MC, Herbet, G, Moritz-Gasser, S, Tate, JE, Duffau, H, 2014. Probabilistic map of critical functions of the human cerebral cortex: Broca's area revisited. Brain 137, 2773–2782. https://doi.org/10.1093/brain/awu168.
Thiebaut de Schotten, M, Tomaiuolo, F, Aiello, M, Merola, S, Silvetti, M, Lecce, F, Bartolomeo, P, Doricchi, F, 2014. Damage to white matter pathways in subacute and chronic spatial neglect: a group study and 2 single-case studies with complete virtual In vivo tractography dissection. Cereb. Cortex 24, 691e706. https://doi.org/10.1093/cercor/bhs351.
Tune, S, Asaridou, SS, 2016. Stimulation the semantic network: what can TMS tell us about the roles of the posterior middle temporal gyrus and angular gyrus. J. Neurosci. 36, 4405–4407. https://doi.org/10.1523/JNEUROSCI.0194-16.2016.
Tzourio-Mazoyer, N, Landeau, B, Papathanassiou, D, et al., 2002. Automated anatomical labelling of activations in SPM using a macroscopic anatomical parcellation of the MNI MRI single-subject brain. Neuroimage 15, 273–289. https://doi.org/10.1006/nimg.2001.0978.
Tzourio-Mazoyer, N, Josse, G, Crivello, F, Mazoyer, B, 2004. Interindividual variability in the hemispheric organization for speech. Neuroimage 21, 422e435.
van de Sandt-Koenderman, ME, van der Meulen, I, Ribbers, GM, 2012. Aphasia rehabilitation: more than treating the language disorder. Arch. Phys. Med. Rehab. 93, S1–S3. https://doi.org/10.1016/j.apmr.2011.08.037.
Vilasboas, T, Herbet, G, Duffau, H, 2017. Challenging the myth of right nondominant hemisphere: lessons from corticosubcortical stimulation mapping in awake surgery and surgical implications. World Neurosurg. 103, 449–456. https://doi.org/10.1016/j.wneu.2017.04.021.
Whitfield-Gabrieli, S, Nieto-Castanon, A, 2012. Conn: a functional connectivity toolbox for correlated and anticorrelated brain networks. Brain Connect. 2, 125–141. https://doi.org/10.1089/brain.2012.0073.
Wilson, SM, Lam, D, Babiak, MC, Perry, DW, Shih, T, Hess, CP, Berger, MS, Chang, EF, 2015. Transient aphasias after left hemisphere resective surgery. Neurosurgery 123, 581–593. https://doi.org/10.3171/2015.4.JNS141962.